

# Hydrodynamic spin fluctuations in the antiferromagnetic Heisenberg chain

Yousef Rahnavard,\* Robin Steinigeweg,† and Wolfram Brenig‡

*Institute for Theoretical Physics, Technical University Braunschweig, D-38106 Braunschweig, Germany*

(Dated: April 16, 2019)

We study the finite temperature, low energy, long wave-length spectrum of the dynamic structure factor of the spin-1/2 antiferromagnetic Heisenberg chain in the presence of exchange anisotropy and external magnetic fields. Using imaginary-time quantum Monte-Carlo we extract parameters, relevant to characterize a *renormalized* Luttinger liquid. For small momentum our results are consistent with a change from propagating spinon density waves to spin diffusion, described by a finite-frequency spin-current relaxation rate. Results for this relaxation rate as well as other Luttinger liquid parameters are presented versus temperature, momentum, magnetic field, and anisotropy, including finite-size analysis, and checks for anomalous diffusion. Our results are consistent with exact diagonalization and Bethe Ansatz, where available, and with corroborate findings of other previous studies using bosonization, transfer matrix renormalization group, and quantum Monte-Carlo.

PACS numbers: 75.10.Jm, 75.40.Gb, 75.50.Ee, 75.40.Mg

## I. INTRODUCTION

The one-dimensional (1D) spin-1/2 antiferromagnetic Heisenberg chain (AFHC) is one of the most fundamental models of quantum many-body physics. It is relevant to low-dimensional magnets,<sup>1</sup> ultra-cold atoms,<sup>2</sup> nanostructures,<sup>3</sup> and – seemingly unrelated – fields such as string theory<sup>4</sup> and quantum Hall systems.<sup>5</sup> In the presence of an external magnetic field, its generalization to anisotropic exchange, the XXZ model, reads

$$H = J \sum_{l=1}^L \left[ \frac{1}{2} (S_l^+ S_{l+1}^- + S_l^- S_{l+1}^+) + \Delta S_l^z S_{l+1}^z - h S_l^z \right], \quad (1.1)$$

where  $J > 0$  is the antiferromagnetic exchange interaction with an anisotropy ratio  $\Delta$ ,  $S_l^{\pm, z}$  are the spin operators on site  $l$  of a chain of length  $L$  with periodic boundary conditions (PBC), and  $B = g\mu_B \hbar h$  is the magnetic field.

Experimentally, dynamical correlation functions of the AFHC have recently become accessible to a variety of high-resolution spectroscopies at finite temperature and in the presence of external magnetic fields, e.g. inelastic neutron scattering (INS),<sup>6–8</sup> high-field nuclear magnetic resonance (NMR),<sup>9–12</sup> muon spin-resonance ( $\mu$ SR),<sup>13</sup> and magnetic transport.<sup>14–16</sup>

Theoretically, and while the AFHC is integrable, its dynamical spin correlation functions remain a major challenge. Analytically, significant progress has been made at low temperatures by calculating multi-spinon response functions<sup>17</sup> from Bethe Ansatz, including the cases of  $h \neq 0$  and  $\Delta \neq 1$ . Important insight has also been obtained in the continuum limit and at low temperatures by bosonization.<sup>18,19</sup> Perturbation theory allows to access regimes of  $\Delta \gg 1$ .<sup>20</sup> Numerically, at finite temperature, time-dependent density-matrix renormalization group (t-TDMRG)<sup>21</sup> is a very powerful approach. However, at present, entanglement growth remains a limiting factor on the time window to access low-energy, long-wavelength dynamics.<sup>22,23</sup> Recently, dy-

namical quantum typicality (t-QT) has been shown to overcome such limitations,<sup>24–26</sup> however, only at high temperatures. Early on, exact diagonalization<sup>27–29</sup> and, more recently, Lanczos variants<sup>30</sup> have been used. However, finite-size or Krylov-space-dimension effects limit their spectral resolution.

Quantum Monte-Carlo (QMC) is an additional complementary approach for the AFHC. It is applicable from low to high temperatures and allows to consider systems almost in the thermodynamic limit, including finite magnetic fields and anisotropy. *Static* correlation functions can be obtained from it with arbitrary precision, however, the evaluation of spin *spectra* from QMC<sup>31–34</sup> requires analytic continuation of imaginary-time data, leading to errors from maximum-entropy approaches.<sup>35</sup> This renders the evaluation of the dynamic structure factor  $S(q, \omega)$  by QMC very challenging, in particular for small momenta  $q \ll 1$ , where sharp low-energy spectral features are expected. Recently therefore, QMC results<sup>36</sup> for  $S(q, \tau)$  at imaginary time  $\tau$  have been compared directly to suggestions from bosonization and time-dependent transfer-matrix renormalization group (t-TMRG),<sup>37,38</sup> corroborating a picture of finite-temperature *diffusive* spin dynamics at finite frequencies in the low-energy, long-wavelength limit. Such spin diffusion in the AFHC is a long-standing issue,<sup>40</sup> relating the magnetization dynamics to the question of dissipation of spin currents and the quest for a spin-Drude weight in the XXZ model, see e.g. Ref. 25 and references therein.

In this context, the aim of the present work is to extend the information obtained from the QMC approach of Ref. 36 into various directions, including physical as well as technical aspects. The manuscript is organized as follows. In Sec. II, we describe our method of analysis. In Sec. III we revisit Ref. 36 from three directions, first, by subjecting its findings to a finite-size scaling analysis, second, by comparing our extended results with exact diagonalization, and third, by checking for anomalous corrections to diffusion. The following Secs. IV and V extend the analysis in two additional ways, namely, by studying the

impact of finite magnetic fields and anisotropy. Section VI summarizes our findings.

## II. QMC APPROACH

The prime object of interest in this work is the Fourier transform of the *longitudinal* dynamic structure factor

$$S(q, \omega) = \int_{-\infty}^{\infty} dt e^{i\omega t} S(q, t) \quad (2.1)$$

at small momentum  $q$  and frequency  $\omega$ , and its corresponding retarded dynamical spin susceptibility  $\chi_{\text{ret}}(q, \omega) \equiv \chi' + i\chi''$  is related to  $S(q, \omega)$  by the fluctuation-dissipation theorem  $\chi''(q, \omega) = [1 - \exp(-\beta\omega)]S(q, \omega)/2$  at inverse temperature  $\beta = 1/T$ . Here  $t$  refers to real time and  $S(q, t) = \langle S_q^z(t) S_{-q}^z \rangle$  with  $S_q^z = \sum_l e^{-iq_l} S_l^z$  being the spin  $z$  component at momentum  $q$ .

$S(q, \omega)$  is related to the imaginary-time structure factor  $S(q, \tau) = \langle S_q^z(\tau) S_{-q}^z \rangle$  by analytic continuation through the usual integral transform  $S(q, \tau) = \int_0^{\infty} d\omega K(\omega, \tau) S(q, \omega) / \pi$  with a kernel  $K(\omega, \tau) = e^{-\tau\omega} + e^{-(\beta-\tau)\omega}$ . While QMC allows to evaluate  $S(q, \tau)$  with high precision, inverting the latter integral transform, e.g. by maximum entropy methods,<sup>35</sup> is mathematically ill-posed and introduces errors which can be considerable in particular at small  $q$  and  $\omega$ .<sup>34</sup> A central point of the present work is, that instead of performing such analytic continuation, we follow<sup>36</sup> and express  $\chi(q, \omega)$  through only a few relevant parameters, by fitting numerical imaginary-time QMC data to an educated analytic guess for  $\chi(q, \tau)$ . While this avoids errors from analytic continuation, it obviously represents a bias which requires *posteriori* quality checks.

Throughout this paper we will be interested in the long-wavelength, low-energy limit, and in a temperature range where we may assume that the physics of Eq. (1.1) can be described by a *renormalized* Luttinger liquid (LLQ). Therefore we start from

$$\chi_{\text{ret}}(q, \omega) = \frac{Kvq^2/2\pi}{\omega^2 - v^2q^2 - \Pi_{\text{ret}}(q, \omega)}. \quad (2.2)$$

Except for  $\Pi_{\text{ret}}$ , this form of  $\chi_{\text{ret}}$  is dictated by the response of a *free* LLQ with Luttinger parameter  $K$  and spinon velocity  $v$ . All deviations from the free LLQ are encapsulated in the irreducible density self-energy  $\Pi_{\text{ret}}(q, \omega)$ . Causality requires that the real(imaginary) part of the latter is an even(odd) function in  $\omega$ . Assuming that  $\Pi_{\text{ret}}(q, \omega)$  is non-singular for small  $\omega$ , and since we are interested in the low- $\omega$  limit, we expand to  $O(\omega^2)$

$$\Pi_{\text{ret}}(q, \omega) \simeq u_0(q) + iu_1(q)\omega + u_2(q)\omega^2 + \dots \quad (2.3)$$

with  $u_i(q) \in \mathbb{R}$ . Expanding also to  $O(q^2)$  for  $q \ll 1$ , inversion symmetry forces

$$\Pi_{\text{ret}}(q, \omega) \simeq c v^2 q^2 - 2i\gamma\omega - b\omega^2 + \dots \quad (2.4)$$

with *real* constants  $c$ ,  $\gamma$ , and  $b$ , and all terms of order higher than  $\omega^2$ ,  $q\omega$ , and  $q^2$  have been dropped. Since we will confine ourselves to  $|\Delta| \leq 1$  and the longitudinal dynamical structure below the saturation field  $h \leq h_c = 2$  we may discard terms constant in  $q$  and  $\omega$  in Eq. (2.4), since they would lead to a gap in  $\chi_{\text{ret}}(0, \omega)$ .

We emphasize, that Eq. (2.4) follows solely from causality, analyticity, and symmetry. Therefore, bosonizing the HAFc and performing proper perturbation theory beyond the free LLQ *must* result in exactly this small  $q, \omega$  expansion for  $\Pi_{\text{ret}}(q, \omega)$ . This is consistent with Refs. 18, 19, 37, and 38, where explicit expressions for  $c$ ,  $\gamma$ , and  $b$  have been obtained to second order in Umklapp scattering and first order in band curvature. In contrast to this perturbation theory however, the spirit of our work is very different. In fact we will view  $v$ ,  $K$ ,  $c$ ,  $\gamma$ , and  $b$  as *parameters* to be determined by fitting to imaginary-time QMC results for  $\chi(q, \tau)$ . This is a non-perturbative approach. To this end we map Eqs. (2.2), (2.4) onto bosonic Matsubara frequencies  $\omega_n = 2\pi nT$  with integer  $n$ ,

$$\chi(q, \omega_n) = \frac{K_q v_q q^2 / (2\pi)}{(1+b)\omega_n^2 + (1+c)v_q^2 q^2 + 2\gamma_q |\omega_n|}, \quad (2.5)$$

and transform this to imaginary time with

$$\chi(q, \tau) = 2 \sum_{n=0}^{\infty} \cos(\omega_n \tau) \chi(q, \omega_n) - \chi(q, 0), \quad (2.6)$$

Several comments are in order. First, the static susceptibility  $\chi_q = \chi_q(q, 0)$  of the XXZ model is known to vary with  $q$ , e.g., at  $\Delta = 1$  and  $h = 0$  it increases monotonously as  $q \rightarrow \pi/2$ . However,  $\chi_q = K/[2\pi v(1+c)]$  resulting from Eqs. (2.2), (2.4) is momentum-independent. To fix this shortcoming of the free LLQ theory, we allow for an additional momentum dependence  $K \rightarrow K_q$ ,  $v \rightarrow v_q$  in Eq. (2.5) - albeit weak at  $q \ll 1$  -, when matching Eqs. (2.2), (2.4) with QMC. Second, the constants  $b$  and  $c$  in Eq. (2.4) are redundant when fitting to QMC because they can always be absorbed into a renormalization of  $K_q$ ,  $v_q$ , and  $\gamma$ . Without loss of generality we therefore fix  $b$  and  $c$ <sup>41</sup> to the values obtained from the perturbation theory of Refs. 18, 19, 37, and 38. Third, as an additional generalization of Eq. (2.4) we allow for a momentum dependence  $\gamma \rightarrow \gamma_q$ . Fourth, Eq. (2.2) with Eq. (2.4) does not capture the finite width of the spectral function  $\chi''(q, \omega)$  at  $T = 0$ , resulting primarily from the two-spinon continuum. However, at  $q/\pi \ll 1$  the latter width is of order  $Jq^3$ , which is negligible against  $\gamma_q$  for those wave vectors and temperatures which we will be interested in.

In summary, our procedure consists in evaluating  $\chi(q, \tau)$  by QMC and fitting the result at each  $q$ , using Eq. (2.6), in terms of three numbers:  $K_q$ ,  $v_q$ , and  $\gamma_q$ .

### A. Spin Diffusion

For finite  $\gamma_q$  and  $\omega \ll \gamma_q$ , Eq. (2.2) displays a diffusion pole with a diffusion constant  $\Gamma_q = (1 +$

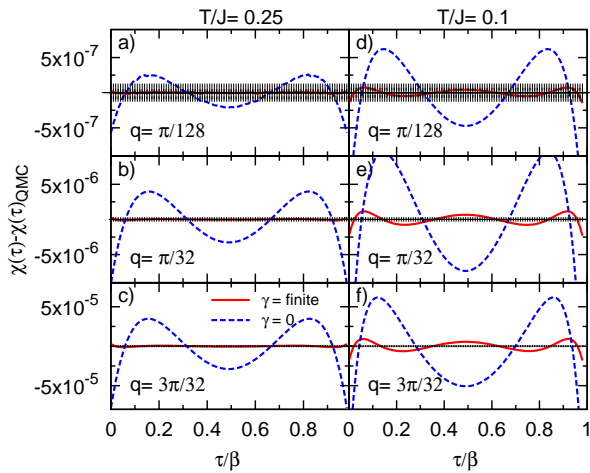


FIG. 1. (color online) Differences between the fitted curves and the original QMC results at the isotropic point for different wave vectors and temperatures. The system-size considered here is  $L = 256$ . Error bars shown in the figure indicate the statistical noise of the QMC data.

$c)v_q^2/(2\gamma_q)$ . Therefore the prime effect of the renormalization  $\Pi_{\text{ret}}(q, \omega)$ , which we study in this work, is to generate a hydrodynamic regime in which the magnetization dynamics of the HAFC is diffusive. This also has consequences for the *regular* spin conductivity  $\sigma_{\text{reg}}(\omega)$ , which we sketch briefly next.

The spin current is defined by the lattice version of the continuity equation  $\partial_t S_q^z = [1 - \exp(-iq)]j_q$ , and its conductivity  $\sigma(\omega) = (1 - e^{\beta\omega})\text{Re} \int_{-\infty}^{\infty} e^{i\omega t} \langle j_0(t)j_0 \rangle dt / \omega$  can be decomposed as

$$\sigma(\omega) = D\delta(\omega) + \sigma_{\text{reg}}(\omega), \quad (2.7)$$

where  $D$  is the enigmatic spin Drude weight and  $\sigma_{\text{reg}}(\omega)$  is the regular part of the spin conductivity. The Drude weight of the HAFC has been of interest for more than two decades by now. We refer to Ref. 25 for the recent status. The regular conductivity is related to the spectrum  $\chi''(q, \omega)$  through the continuity equation

$$\sigma_{\text{reg}}(\omega) = \lim_{q \rightarrow 0} \frac{\omega}{q^2} \chi''(q, \omega). \quad (2.8)$$

If  $\chi(q, \omega)$  exhibits a diffusion pole in the frequency domain, then in the time domain Eq. 2.8 implies exponential decay of the current on a time scale  $1/\gamma_0$  given by the current relaxation rate  $\gamma_0$ .<sup>39</sup> In the frequency domain it implies a Lorentzian line shape of  $\sigma_{\text{reg}}(\omega)$  with width  $\gamma_0$ . We emphasize that Eq. (2.8) provides *no* insight into the value of  $D$ . Coexistence of a diffusive regular conductivity with a finite Drude weight has been suggested based on bosonization, t-TMRG, and memory-function methods.<sup>37,38</sup> But also strong momentum dependence beyond Eq. (2.4) has been invoked to question this, based however on small systems at high temperatures.<sup>30</sup> For the

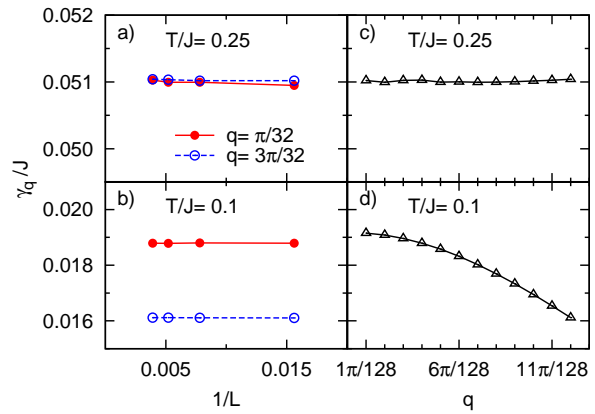


FIG. 2. (color online) Finite-frequency spin-current relaxation rate  $\gamma_q$  of the isotropic Heisenberg spin chain versus inverse system-size  $1/L$  and momentum  $q$  for chain lengths  $64 < L < 256$  at two temperatures  $T/J = 0.1, 0.25$ . For momentum dependence of  $\gamma_q$ , the largest system-size  $L = 256$  is chosen.

remainder of this work we will refrain from speculations on  $D$ .

### III. ISOTROPIC CHAIN

In this section we extend previous work,<sup>36</sup> based on the approach described in Sec. II, into several new directions. First we study the effects of system-size. Then we perform a consistency check of our approach by comparing to available results from exact diagonalization. Finally, we test if the current relaxation rate shows relevant energy dependence.

#### A. System-size and momentum dependence

In Ref. 36, the approach described in the previous section has been applied to the isotropic HAFC, i.e. at  $\Delta = 1$  and  $h = 0$ . That work has proven feasibility of the method. In particular it was shown, that  $K_0$  and  $v_0$  extracted from it agree very well with thermodynamic Bethe Ansatz,<sup>42,43</sup> as well as that the relaxation rate  $\gamma_0$  obtained was consistent with that from bosonization and t-TMRG<sup>37,38</sup> to within factors of 2. We will not repeat this analysis here. Instead we note that the findings of Ref. 36 were based on a *single* system-size, i.e.  $L = 128$ , and it remained unclear if parts of its results, e.g. the momentum dependencies observed for  $\gamma_q$  were finite-size effects. Therefore, in this subsection, we will analyze  $\gamma_q$  versus system-size.

To begin we comment on the accuracy of the fitting procedure summarized in the last paragraph before Sec. II A. To this end Fig. 1 shows the minimum difference between our QMC results and Eq. (2.6) for optimized

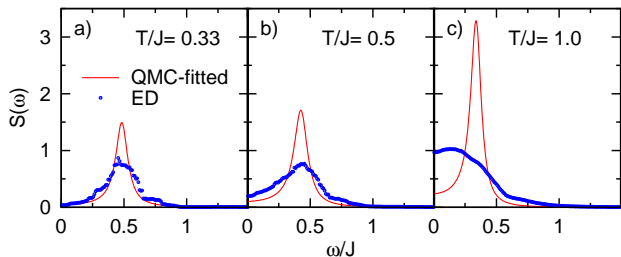


FIG. 3. (color online) Hydrodynamic spectra in the frequency domain with parameters fitted to QMC as compared to ED, both for length  $L = 18$ , momentum  $q = \pi/9$ , the isotropic point  $\Delta = 1$ , and three temperatures  $T/J = \{0.33, 0.5, 1.0\}$ .

parameters  $K_q$ ,  $v_q$ , and  $\gamma_q$ , for different temperatures and small, nonzero wave vectors on a system with 256 sites. In addition each panel also shows this difference assuming that  $\gamma_q = 0$ , i.e. discarding spin diffusion. The figure also displays the statistical noise of the QMC data as error bars. Several points have to be mentioned. First, the quality of our imaginary-time QMC results is worth noting by observing the absolute order of magnitude on the  $y$  axes of this figure. Second, for all panels shown, including a finite  $\gamma_q$  leads to clearly better agreement with QMC than setting  $\gamma_q = 0$ . We emphasize, that  $\gamma$  is  $\sim O(J/20 \dots 100)$ , which implies that our method is capable to sense spectral structures on such small energy scales. This is unlikely for standard maximum-entropy analytic continuation. Third, at intermediate temperatures,  $T = 0.25J$ , using Eqs. (2.2), (2.4) with finite  $\gamma_q$  is well within the standard deviation of QMC for all momenta depicted. For lower temperatures this is so at least for the smallest momenta, i.e. as  $q \rightarrow 0$ . Therefore these plots also show that, while a finite  $\gamma_q$  clearly improves agreement with QMC, the range of validity in momentum space of the purely hydrodynamic, diffusive description shrinks as the temperature is lowered. Similar observations have been made in Ref. 40. Future work should elaborate on this. Finally, the figure shows that  $\gamma_q$  decreases with temperature.<sup>36–38</sup>

Next we turn to the system-size dependence of  $\gamma_q$ . To that end we consider four chains with sizes of  $L = 64, 128, 192, 256$ . The results are shown in Fig. 2 a), b) for two different temperatures  $T/J = 0.1, 0.25$  and two momenta. Note that these momenta,  $q = \pi/32, 3\pi/32$ , have been chosen to be identical despite the differing system-sizes, which implies that they are not necessarily the smallest wave vector possible for a given  $L$ . The main point of this figure is, that we observe *no* finite-size dependence. This is even more so in view of the  $y$  axes scales depicted. Therefore our results can safely be considered as being in the thermodynamic limit.

In panels c), d) of this figure we show  $\gamma_q$  versus momentum for the largest system, i.e.,  $L = 256$ . Obviously, for the lower temperature  $T = 0.1$ ,  $\gamma_q$  slightly decreases with  $q$ .<sup>44</sup> This is fully identical to the findings of Ref.

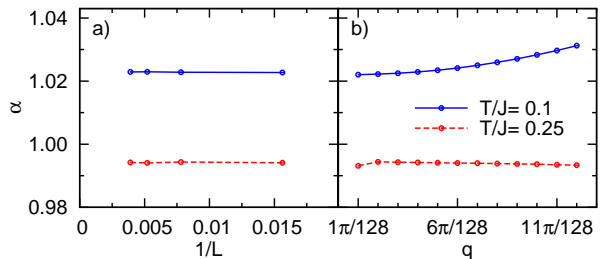


FIG. 4. (color online) Exponent  $\alpha$  of the spin-density relaxation rate  $\gamma\omega^\alpha$  of the isotropic Heisenberg chain versus a) inverse system-size  $1/L$  at momentum  $q = \pi/32$  of system-sizes  $64 < L < 256$ , b) momentum  $q$  for a system-size of  $L = 256$ . In both panels, two temperatures  $T/J = 0.25, 0.1$  are considered.

36, where however  $L = 128$  was used. I.e. this decrease is not a finite-size effect as was speculated in the latter work. Rather, and in view of the deviation in Fig. 1 e), f), we believe that the crossover from a constant to a weakly momentum-dependent  $\gamma_q$  is another indication of a shrinking hydrodynamic regime as the temperature is lowered.

## B. Comparison with exact diagonalization

Apart from Fig. 1, another quality check of our method can be constructed by comparison with results from exact diagonalization (ED). While the latter are beyond any doubt, they can only be obtained on small systems, in particular if complete diagonalization is performed using a canonical ensemble. Small system-sizes imply that the smallest, nonzero wave vectors remains rather large, and moreover, that acceptably smooth spectra can only be obtained for rather large temperatures. Nevertheless, it is very tempting to compare our QMC approach with ED results.

Figure 3 compares the evolution with temperature of the longitudinal structure factor  $S(q, \omega)$ , obtained from both, the QMC method of Sec. II and ED on chains of identical length, i.e.  $L = 18$ , at the smallest, nonzero wave vector  $q = \pi/9$ . This comparison is remarkable. First, it is obvious, that as  $T$  is lowered, the agreement between ED and the QMC approach improves monotonously. At the lowest temperature the width of the two spectra are almost identical. The peak heights are still different. We attribute this to two effects. First, at low temperature respective finite-size effects are more prominent. Second, the width of the ED spectrum is still slightly larger than that of QMC. In turn, sum-rule effects will decrease the ED's peak intensity. As we increase  $T$  the line shape of the ED clearly broadens beyond that of the QMC at  $T/J = 0.5$ , and for  $T/J = 1.0$  the agreement is lost.

Exactly this variation with temperature is expected.

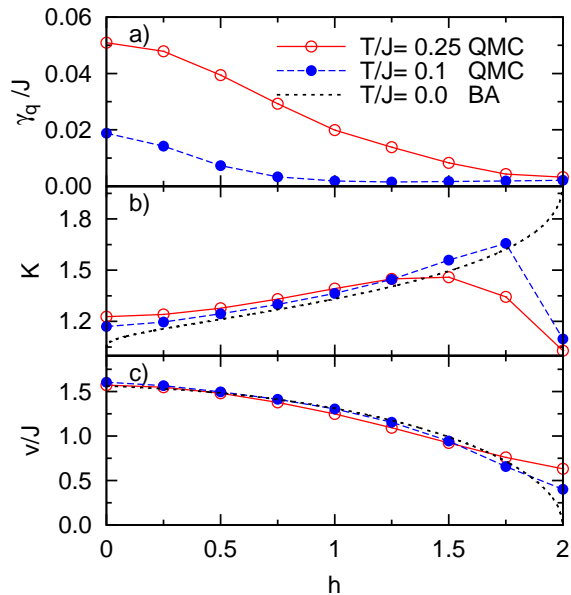


FIG. 5. (color online) a) Spin current relaxation rate  $\gamma_q$ , b) Luttinger parameter  $K$ , and c) spin velocity  $v$  at finite temperatures  $T/J = 0.1, 0.25$  obtained from QMC of a chain with 64 sites. Luttinger parameter  $K$  and spin velocity  $v$  at zero temperature known from BA in terms of magnetic field are also shown. In the case of QMC, the momentum is  $q = \pi/32$ .

For low  $T$  a description of the HAFC in terms of a renormalized LLQ should hold, explaining the rather similar spectra from ED and our QMC approach. We speculate that this agreement should even improve for  $T < 0.33J$ , where however ED spectra are too noisy. Increasing the temperature, it is known that up to  $T/J \lesssim 0.1$  perturbatively renormalized LLQs provide a good description of *thermodynamic* properties of the HAFC which agree rather well with static QMC or TBA,<sup>1,42</sup> while for  $T/J \gtrsim 0.25$  the agreement starts to deteriorate. In view of this breakdown of the LLQ description, it is natural that ED and our QMC approach start to differ for  $T/J > 0.5$ , as in Fig. 3.

### C. Anomalous diffusion

As a final check we test the stability of our approach against modifications of the basic diffusion law by super(sub)diffusion. The latter is defined by a density which spreads in time according to  $\langle r^2 \rangle \sim t^\alpha$  with  $\alpha > 1 (< 1)$ . In terms of Eq. (2.4), this implies a substitution

$$\gamma\omega \rightarrow \gamma\omega^\alpha \quad (3.1)$$

with  $\alpha \neq 1$ . Recently, anomalous diffusion has been claimed to result from Lindblad quantum master equations at the isotropic point and infinite temperatures.<sup>45,46</sup>

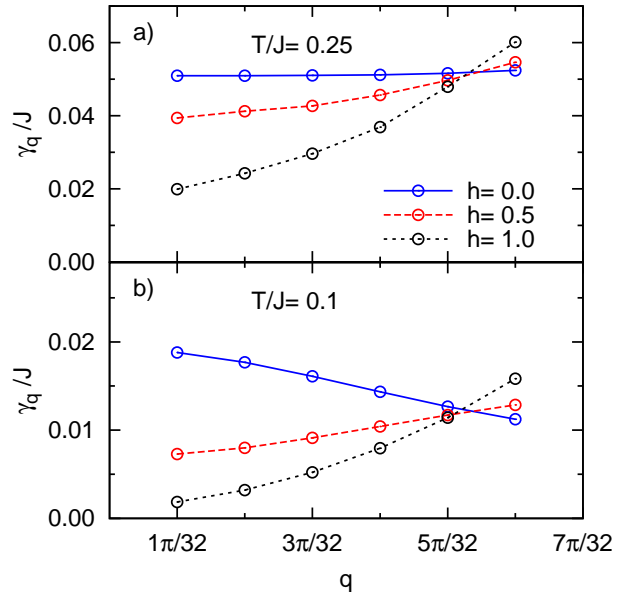


FIG. 6. (color online) Momentum dependence of the spin current relaxation rate for two temperatures a)  $T/J = 0.25$ , b)  $T/J = 0.1$ , and different external magnetic fields is plotted. The system-size considered here is  $L = 64$ .

This claim is consistent with numerical simulations of spin-density dynamics on the basis of classical mechanics.<sup>52</sup>

Allowing for the modification of Eq. (3.1) within our approach is straightforward and leads to one additional fitting parameter. The results for  $\alpha$  at two temperatures  $T = 0.1J, 0.25J$  are summarized in Fig. 4. Panel a) of this figure depicts finite-size scaling of  $\alpha$  for system-sizes  $64 < L < 256$  and one momentum  $q = \pi/32$ .  $\alpha$  versus momentum for a system-size of  $L = 256$  is shown in panel b) of this figure. To summarize,  $\alpha$  remains very close to one, i.e. any tendencies towards super(sub)diffusion at low temperatures are negligible and can safely be discarded. We note in passing, that all modifications we observe in  $K_q, v_q$  and  $\gamma_q$ , due to allowing for  $\alpha \neq 1$ , are also negligible.

### IV. MAGNETIC FIELD DEPENDENCE

In this section, we will extend our approach to the case of finite magnetic fields in the isotropic chain. Since we consider the longitudinal dynamical structure factor, the spectrum remains gapless below the saturation field  $h_c = 2$ .

First, Fig. 5a) shows  $\gamma_q$  versus field for two temperatures  $T = 0.1, 0.25 J$  at wave vector  $q = \pi/32$  in a system with  $L = 64$ . This evidences a monotonous decrease of the relaxation rate with magnetic field. Such a behavior is consistent with predictions at low fields from bosonization.<sup>38</sup> While overlap between the spin current and the conserved heat current of the HAFC at

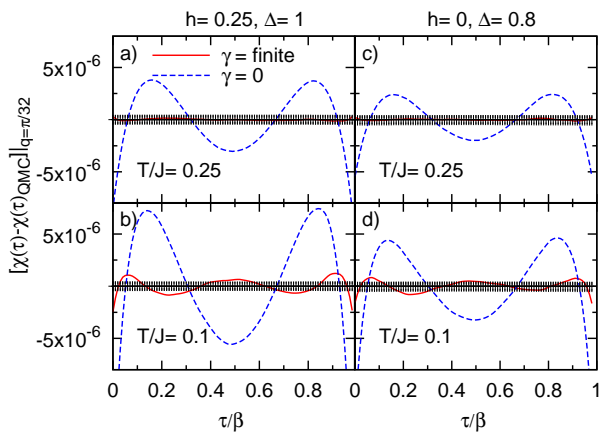


FIG. 7. (color online) Differences between the fitted curves and original QMC data at momentum  $q = \pi/32$  and two temperatures  $T/J = 0.25, 0.1$ . In panels a) and b), magnetic field is set to  $h = 0.25$  and anisotropy is set to  $\Delta = 1$  while in panels c) and d),  $h = 0$  and  $\Delta = 0.8$ . The system-size for all cases is  $L = 64$  and the error bars indicate the statistical noise of the QMC data.

nonzero  $h$  irrevocably imply a finite spin Drude weight for  $0 < h < h_c$ ,<sup>47–49</sup> this allows for no conclusion on the regular conductivity  $\sigma_{\text{reg}}(\omega)$  from Eqs. (2.7), (2.8). In Refs. 37 and 38 this has been dubbed coexistence of ballistic and diffusive transport channels, meaning that in the time domain, and on relatively short scales, currents relax diffusively onto a constant infinite-time limiting value. Therefore, while our nonzero  $\gamma_q$  does not contradict a finite Drude weight, it is nevertheless reassuring that the decrease of  $\gamma_{q_{\text{min}}}$  we observe is indicative of a ‘more’ ballistic behavior of the system as  $h$  increases.

Next we turn to the remaining two fitting parameters  $K_q$  and  $v_q$ . As the magnetic field sets the chemical potential of the Jordan-Wigner fermions, it is clear that apart from changes in  $\gamma_q$  versus  $h$  we also expect the LLQ parameters  $K_q$  and  $v_q$  to be sensitive to  $h$ . This is shown in Fig. 5b) and c) for the same wave vector and temperatures as in panel a). At  $T = 0$  the LLQ parameters can be obtained from Bethe Ansatz (BA).<sup>50</sup> Regarding our approach it is very satisfying to see that  $K_q$  and  $v_q$  almost quantitatively agree with BA, and moreover that the remaining discrepancies diminish as  $T \rightarrow 0$  in the QMC approach. We emphasize that it should come as no surprise, that expectation values obtained from *static* QMC agree with other exact methods. Rather the main point is that  $K_q$  and  $v_q$  within our QMC approach follow from fits to a *dynamic* structure factor. We note that the downturn of  $v_q$  with  $h$  is consistent with the physical picture of a cosine band being filled completely as  $h \rightarrow h_c$ .

Figure 6 displays  $\gamma_q$  versus momentum for two temperatures  $T = 0.1, 0.25 J$  and various magnetic fields  $h = 0, 0.5, 1.0$ , up to half of the saturation field. This figure shows, that increasing  $h$  decreases the slope of  $\gamma_q$  and modifies the curvature as well. However,  $\gamma_q(h > 0)$  is not

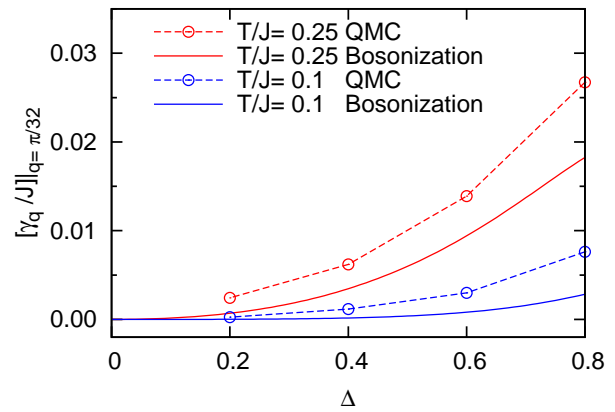


FIG. 8. (color online) Anisotropy dependence of the spin-current relaxation rate obtained from bosonization (solid curves) and our method (symbols) for two temperatures  $T/J = 0.1, 0.25$ . For QMC, the first nonzero momentum  $q = \pi/32$  on a system of length  $L = 64$  is considered.

less than  $\gamma_q(h = 0)$  for large momenta. To gauge if the introduction of  $\gamma_q$  improves the agreement between the renormalized LLQ and the imaginary-time QMC data, as compared to the free LLQ, also for finite magnetic fields, we display the difference between  $\chi(q, \tau)$  from Eq. (2.5) and that obtained from QMC in Fig. 7a) and b). This figure clearly supports  $\gamma_q \neq 0$ . Similar however to the zero-field case, the QMC data also suggests that at low temperatures, additional, albeit smaller, renormalizations beyond diffusion are present.

## V. ANISOTROPY

Finally, we consider the role of finite anisotropy for the range of  $0 < \Delta < 1$ . To this end Fig. 8 displays the relaxation rate versus  $\Delta$  for two temperatures  $T/J = 0.1$  and  $0.25$  obtained from two methods, i.e. our QMC approach and the perturbation theory based on bosonization.<sup>37,38</sup> For QMC the results are plotted for the smallest, nonzero wave vector on a chain of length  $L = 64$ , i.e.  $q = \pi/32$ . The bosonization result is of the form  $\gamma(T) = f(K, v)T^{4K-3}$ , where  $f$  is a function of the Luttinger parameter  $K$  and the spin velocity  $v$  which are exactly known from BA at zero temperature. This figure shows, that the QMC results behave qualitatively very similar to the findings from bosonization yet, QMC is consistently larger than the latter. The figure does not show the point  $\Delta = 1$ , since at that point a similar comparison has already been performed in Ref. 36. The evolution of  $\gamma_q$  with  $\Delta$  as the latter approaches zero is very much consistent with the fact that at  $\Delta = 0$  the HAFc is in the XY limit, i.e. a free Fermi gas, which displays fully ballistic spin transport, i.e.  $\gamma = 0$ .

As for the case of finite magnetic fields, in Fig. 9 we now turn to the dependence of the two LLQ parameters

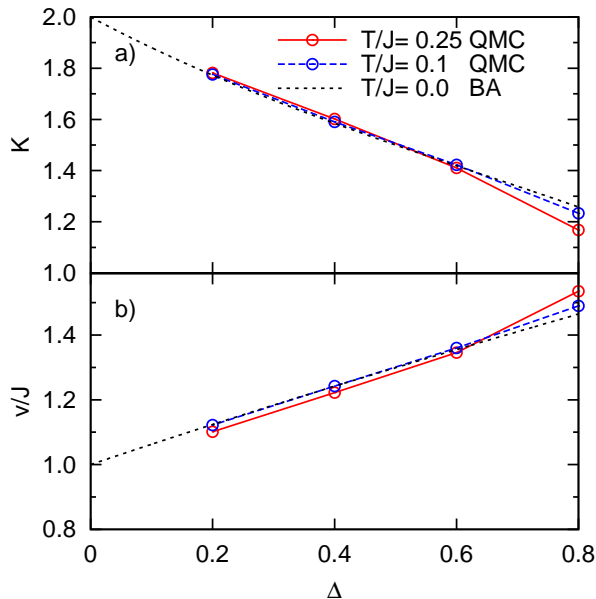


FIG. 9. (color online) a) Luttinger parameter and b) spin velocity at finite temperature obtained from QMC in terms of anisotropy for the first nonzero momentum at chain length  $L = 64$ . Luttinger parameter and spin velocity at zero temperature known from BA are also shown for comparison purposes.

$K_q$  and  $v_q$  for the smallest wave vector on a  $L = 64$  site chain. Once again, values for these parameters at  $T = 0$  are known from BA, i.e.

$$K = \frac{\pi}{\pi - \arccos \Delta}, \quad v = \frac{\pi \sqrt{1 - \Delta^2}}{2 \arccos \Delta}. \quad (5.1)$$

In Fig. 9 results from the fits to QMC are compared with BA. As for the finite field we observe very good agreement, which improves as  $T \rightarrow 0$ .

As for the previous sections, we also consider the effects of anisotropy on the momentum dependence of the relaxation rate. This is shown in Fig. 10 at two temperatures  $T = 0.1, 0.25 J$  for the isotropic point  $\Delta = 1$  and two values of anisotropy  $\Delta = 0.2, 0.6$ . Similar to the finite-field case, the slope and curvature of  $\gamma_q(\Delta)$  versus  $q$  varies with  $\Delta$ , albeit less strong. For the higher temperature, i.e.  $T = 0.25 J$ , only a weak momentum dependence can be observed at the isotropic point and an increasing function in the anisotropic case. For  $T = 0.1 J$ ,  $\gamma_q$  decreases with  $q$  at  $\Delta = 1$ , while for the anisotropic case, this behavior is reversed.

The quality of the QMC fits to Eq. (2.6) for a finite  $\Delta = 0.8$  are depicted in Fig. 7. They exhibit the same trend as in all similar comparisons discussed in this work, i.e. a finite  $\gamma$  clearly improves agreement with QMC as compared to  $\gamma = 0$ , with however systematic deviations still present for very low temperatures and finite momenta.

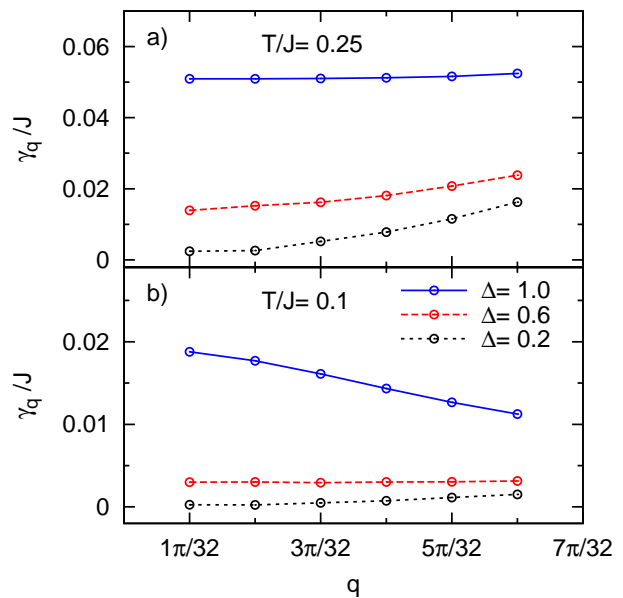


FIG. 10. (color online) Momentum dependence of the spin-current relaxation rate  $\gamma_q$  for different anisotropies  $\Delta = 1.0, 0.6, 0.2$  at two temperatures a)  $T = 0.25J$  and b)  $T = 0.1J$ . The system-size here is set to  $L = 64$ .

## VI. SUMMARY

In summary, we have explored the dynamic structure factor of the antiferromagnetic Heisenberg chain at long wave lengths and finite temperatures. For this we have used the response function of a Luttinger liquid including self-energy corrections which were parametrized in terms of only a few relevant parameters. We have then determined these parameters by fitting to high-precision imaginary-time quantum Monte-Carlo calculations. Quite generically we find, that the self-energy renormalizes the low-energy, long wavelength density spectrum of the Luttinger liquid from a propagating ‘sound’ mode into a diffusion mode. Apart from the standard Luttinger parameters, the diffusion mode introduces one additional parameter, i.e. a current relaxation rate. We have analyzed this relaxation rate with respect to several physical variables: temperature, momentum, magnetic field, and anisotropy. Moreover, we have shown consistency of our approach by performing finite-size analysis, checking for anomalous diffusion, and comparing with exact diagonalization and results from Bethe Ansatz. Our findings are qualitatively consistent with previous studies using perturbation theory and bosonization, as well as with a limited QMC analysis, considering only the role of temperature and momentum for a single system-size. Future work should enlarge the variational space for the self-energy, in order to capture corrections to purely diffusive behavior.

*Note added:* After completion of this work we have become aware of very recent results,<sup>51</sup> obtained in a differ-

ent context, with different methods, which are also consistent with a finite zero-frequency limit of the regular spin conductivity in the HAFC.

### ACKNOWLEDGMENTS

We thank P. Prelovšek, X. Zotos, and J. Herbrych for very helpful discussions. Part of this work has been sup-

ported by the Deutsche Forschungsgemeinschaft through FOR912, grant no. BR 1084/6-2, the European Commission through MC-ITN LOTHERM, grant no. PITN-GA-2009-238475, and the NTH School for Contacts in Nanosystems. W.B. thanks the Platform for Superconductivity and Magnetism Dresden, where part of this work has been performed, for its kind hospitality.

- 
- \* y.rahnvard@tu-bs.de  
† r.steinigeweg@tu-bs.de  
‡ w.brenig@tu-bs.de
- 1 D. C. Johnston, R. K. Kremer, M. Troyer, X. Wang, A. Klümper, S. L. Bud'ko, A. F. Panchula, and P. C. Canfield, *Phys. Rev. B* **61**, 9558 (2000).
  - 2 S. Trotzky, P. Cheinet, S. Fölling, M. Feld, U. Schnorrberger, A. M. Rey, A. Polkovnikov, E. A. Demler, M. D. Lukin, and I. Bloch, *Science* **319**, 295 (2008).
  - 3 P. Gambardella, *Nature Mat.* **5**, 431 (2006).
  - 4 M. Kruczenski, *Phys. Rev. Lett.* **93**, 161602 (2004).
  - 5 Y. B. Kim, *Phys. Rev. B* **53**, 16420 (1996).
  - 6 M. B. Stone, D. H. Reich, C. Broholm, K. Lefmann, C. Rischel, C. P. Landee, and M. M. Turnbull, *Phys. Rev. Lett.* **91**, 037205 (2003).
  - 7 B. Lake, D. A. Tennant, C. D. Frost, and S. E. Nagler, *Nature Mat.* **4**, 329 (2005).
  - 8 M. Mourigal, M. Enderle, A. Klöpperpieper, J.-S. Caux, A. Stunault, H. M. Rønnow, *Nature Phys.* **9**, 435 (2013).
  - 9 M. Takigawa, O. A. Starykh, A. W. Sandvik, and R. R. P. Singh, *Phys. Rev. B* **56**, 13681 (1997).
  - 10 K. R. Thurber, A. W. Hunt, T. Imai, and F. C. Chou, *Phys. Rev. Lett.* **87**, 247202 (2001).
  - 11 A. U. B. Wolter, P. Wzietek, S. Süllow, F. J. Litterst, A. Honecker, W. Brenig, R. Feyerherm, and H.-H. Klauss, *Phys. Rev. Lett.* **94**, 057204 (2005).
  - 12 H. Kühne, H.-H. Klauss, S. Grossjohann, W. Brenig, F. J. Litterst, A. P. Reyes, P. L. Kuhns, M. M Turnbull, and C. P. Landee, *Phys. Rev. B* **80**, 045110 (2009).
  - 13 F. L. Pratt, S. J. Blundell, T. Lancaster, C. Baines, and S. Takagi, *Phys. Rev. Lett.* **96**, 247203 (2006).
  - 14 C. Hess, *Eur. Phys. J. Special Topics* **151**, 73 (2007).
  - 15 F. Heidrich-Meisner, A. Honecker, and W. Brenig, *Eur. Phys. J. Special Topics* **151**, 135 (2007).
  - 16 A. V. Sologubenko, T. Lorenz, H. R. Ott, and A. Freimuth, *J. Low. Temp. Phys.* **147**, 387 (2007).
  - 17 J.-S. Caux *et al.*, *J. Stat. Mech.* **P09003** (2005); *ibid.* **P08006** (2008); *ibid.* **P01007** (2012).
  - 18 R. G. Pereira, J. Sirker, J.-S. Caux, R. Hagemans, J. M. Maillet, S. R. White, and I. Affleck, *J. Stat. Mech.* **P08022** (2007).
  - 19 R. G. Pereira, *Int. J. Mod. Phys. B* **26**, 1244008 (2012).
  - 20 A. J. A. James, W. D. Goetze, and F. H. L. Essler, *Phys. Rev. B* **79**, 214408 (2009).
  - 21 T. Barthel, U. Schollwöck, and S. R. White, *Phys. Rev. B* **79**, 245101 (2009).
  - 22 C. Karrasch, J. H. Bardarson, and J. E. Moore, *Phys. Rev. Lett.* **108**, 227206 (2012).
  - 23 C. Karrasch, J. Hauschild, S. Langer, and F. Heidrich-Meisner, *Phys. Rev. B* **87**, 245128 (2013).
  - 24 T. A. Elsayed and B. V. Fine, *Phys. Rev. Lett.* **110**, 070404 (2013).
  - 25 R. Steinigeweg, J. Gemmer, and W. Brenig, *Phys. Rev. Lett.* **112**, 120601 (2014).
  - 26 R. Steinigeweg, J. Gemmer, and W. Brenig, preprint, arXiv:1408.6837 (2014).
  - 27 K. Fabricius, U. Löw, and J. Stolze, *Phys. Rev. B* **55**, 5833 (1997).
  - 28 R. Werner and A. Klümper, *Phys. Rev. B* **64**, 174414 (2001).
  - 29 O. Waldmann, *Phys. Rev. B* **65**, 024424 (2001).
  - 30 J. Herbrych, R. Steinigeweg, and P. Prelovšek, *Phys. Rev. B* **86**, 115106 (2012).
  - 31 J. Deisz, M. Jarrell, and D. L. Cox, *Phys. Rev. B* **42**, 4869 (1990).
  - 32 J. Deisz, M. Jarrell, and D. L. Cox, *Phys. Rev. B* **48**, 10227 (1993).
  - 33 O. A. Starykh, A. W. Sandvik, and R. R. P. Singh *Phys. Rev. B* **55**, 14953 (1997).
  - 34 S. Grossjohann and W. Brenig, *Phys. Rev. B* **79**, 094409 (2009).
  - 35 M. Jarrell and J.E. Gubernatis, *Phys. Rep.* **269**, 133 (1996).
  - 36 S. Grossjohann and W. Brenig, *Phys. Rev. B* **81**, 012404 (2010).
  - 37 J. Sirker, R. G. Pereira, and I. Affleck, *Phys. Rev. Lett.* **103**, 216602 (2009).
  - 38 J. Sirker, R. G. Pereira, and I. Affleck *Phys. Rev. B* **83**, 035115 (2011).
  - 39 For exceptions from an exponential decay in the case of strong particle-particle interactions  $\Delta > 1$ , see Ref. 40.
  - 40 R. Steinigeweg and W. Brenig, *Phys. Rev. Lett.* **107**, 250602 (2011).
  - 41 E.g. at  $\Delta = 1$ ,  $b = g^2/4 - g^3(3 - 8\pi^2/3)/32 + \sqrt{3}T^2/\pi$  and  $c = g^2/4 - 3g^3/32 - \sqrt{3}T^2/\pi$  in powers of the running coupling constant  $1/g + \ln(g)/2 = \ln(\sqrt{\pi/2} \exp(G + 1/4)/T)$  and  $G \approx 0.577216 \dots$  is Euler's constant.<sup>42</sup>
  - 42 S. Lukyanov, *Nucl. Phys. B* **522**, 533 (1998).
  - 43 A. Klümper and D. C. Johnston, *Phys. Rev. Lett.* **84**, 4701 (2000).
  - 44 Momentum dependence of current relaxation rates has also been studied by Lanczos methods on finite systems up to  $L = 26(28)$  in the zero magnetization sector and at high temperatures  $T = 0.7(10)J$ .<sup>30</sup> This refers to a temperature and momentum range rather different from the hydrodynamic regime we investigate in Fig. 2c), d).
  - 45 M. Žnidarič, *Phys. Rev. Lett.* **106**, 220601 (2011).
  - 46 M. Žnidarič, *Phys. Rev. B* **90**, 115156 (2014).
  - 47 P. Mazur, *Physica (Amsterdam)* **43**, 533 (1969).

- <sup>48</sup> X. Zotos, F. Naef, and P. Prelovšek, Phys. Rev. B **55**, 11029 (1997).
- <sup>49</sup> F. Heidrich-Meisner, A. Honecker, and W. Brenig, Phys. Rev. B **71**, 184415 (2005).
- <sup>50</sup> N. Bogoliubov, A. Izergin, and V. Korepin, Nuclear Physics B **275**, 687 (1986).
- <sup>51</sup> C. Karrasch, D. Kennes, and F. Heidrich-Meisner, preprint, arXiv:1412.6047 (2014).
- <sup>52</sup> R. Steinigeweg, EPL **97**, 67001 (2012).